BioMetals **18:** 31–41, 2005.

The function of Alr1p of *Saccharomyces cerevisiae* in cadmium detoxification: Insights from phylogenetic studies and particle-induced X-ray emission

Ana Lúcia Kern[1,†], Diego Bonatto[1,†], Johnny Ferraz Dias[2], Maria-Lucia Yoneama[3], Martin Brendel[1] & João Antonio Pêgas Henriques[1,*]

[1]*Departamento de Biofísica/Centro de Biotecnologia, UFRGS, Av. Bento Gonçalves 9500, 91507-970 Porto Alegre, RS, Brazil;* [2]*Instituto de Física/UFRGS, Av. Bento Gonçalves 9500, 91501-970 Porto Alegre, RS, Brazil;* [3]*Programa de Pós-Graduação em Geologia, Universidade do Vale do Rio dos Sinos, Caixa Postal 275, CEP 93001-970, São Leopoldo, RS, Brazil; *Author for correspondence (Tel.: 55-51-316-7602; Fax: 55-51-316-6084; E-mail: pegas@dna.cbiot.ufrgs.br)*

Received 15 April 2004; Accepted 5 July 2004; Published online December 2004

Key words: Saccharomyces cerevisiae, phylogenetic analysis, transmembrane transporters, metal uptake, PIXE, hydrophobic cluster analysis

Abstract

Two genes in *Saccharomyces cerevisiae*, *ALR1* and *ALR2,* encode transmembrane proteins involved in Mg^{2+} uptake. The present study investigates the phylogenetic relationship of Alr1p/Alr2p with bacterial CorA proteins and some proteins related to Mg^{2+} influx/efflux transport in mitochondrial and bacterial zinc transporters; including hydrophobic cluster analysis (HCA). The phylogenetic results indicate that the Alrp sequences of *S. cerevisiae* share a common carboxy-terminus with proteins related to zinc efflux transport. We also analyse the intracellular metal content by particle-induced X-ray emission (PIXE) after cell exposure to cadmium. The PIXE analysis of cadmium-exposed *ALR* mutants and wild-type yeast cells suggests that Alrp has a central role in cell survival in a cadmium-rich environment.

Introduction

Heavy metals represent a major environmental hazard to human health. In particular, cadmium (Cd) is very toxic and carcinogenic, even at low concentrations (Trevors *et al.* 1986). The biological effects of this metal and the mechanism of its toxicity are not clearly understood. It has been proposed that Cd^{2+} ions displace Zn^{2+} and Fe^{2+} in proteins (Stohs & Bagchi 1995) and can cause oxidative stress (Brennan & Schiestl 1996), particularly lipid peroxidation (Stohs & Bagchi 1995). More recently, it has been proposed that Cd can bind to DNA bases with little sequence specificity, inducing DNA single-strand breaks and a strong inhibition of the mismatch-repair pathway (McMurray & Tainer 2003). However, many cellular proteins work only in the presence of small amounts of metal ions, such as zinc, iron, copper, manganese, molybdenium, nickel and cobalt (Eide & Guerinot 1997). Therefore, these essential nutrients are actively captured from the environment. During these processes, other metal ions, e.g. heavy metals, can also be absorbed, leading to toxic intracellular concentrations (Eide & Guerinot 1997).

As a survival strategy, all living organisms throughout evolution have developed many mechanisms to minimize heavy metal accumulation (Tomsett & Thurman 1988). These processes are complex in nature and little is known about them. The best understood mechanism is the interaction of thiol-containing amino acids (aa) or peptides with metal ions. The latter can be

[†]Both authors contributed equally to this work.

potentially chelated by thiol-oligopeptides, such as glutathione and phytochelatins (absent in *S. cerevisiae*) or by metallothioneines. Once formed, these complexes can be dislocated to the vacuole or secreted by transmembrane protein transporters (Eide & Guerinot 1997).

It was recently demonstrated that the biological effects of aluminum, an abundant toxic metal element of the Earth's crust (Moeller *et al.* 1984; Pinã & Cervantes 1996), in yeast occurs as a consequence of a reduction of Mg^{2+} influx via Alr proteins. *ALR1* and *ALR2* genes encoded proteins that have a low degree of aa similarity if compared to the CorA Mg^{2+} transport system of bacteria (MacDiarmid & Gardner 1998). Alr1p forms possibly a cation channel located in the yeast plasma membrane and its expression and turnover is controlled by Mg^{2+} concentration (Graschopf *et al.* 2001; Liu *et al.* 2002). The detail of how CorA or Alr proteins work to transport Mg^{2+} into cells is still unclear (Liu *et al.* 2002). Overexpression of *ALR1* and *ALR2* alters the tolerance of *S. cerevisiae* to several metal cations, produces hyper-resistance to Al^{3+} and Ga^{3+} and can also cause hypersensitivity to divalent metal ions such as Co^{2+}, Mn^{2+}, Ni^{2+}, and Zn^{2+} (MacDiarmid & Gardner 1998). Phenotypic analysis of *alr1*Δ and *alr2*Δ mutants of *S. cerevisiae* revealed the importance of the *ALR1* gene, as the *alr1*Δ mutant cannot survive in complete media without an adequate supplement of Mg^{2+} (MacDiarmid & Gardner 1998). This phenotype was seen in *CorA* mutants of the pathogen *Helicobacter pylori*, where the growth arrest in media without a supplement of Mg^{2+} and the drastic Mg^{2+} requirement in the range of 20 mM by CorA mutants, demonstrated the essential *H. pylori* CorA function for Mg^{2+} acquisition in low-Mg^{2+} environments (Pfeiffer *et al.* 2002).

In this work, we analysed the cadmium sensitivity phenotypes and the intracellular level of Cd^{2+} by particle-induced X-ray emission (PIXE) in yeast cells containing a disrupted and a single-copy of *ALR* genes. We also conducted a phylogenetic study of the Alr1p and Alr2p, comparing their primary sequences with those of other divalent cation transporter proteins, mitochondrial Mg^{2+} transporters, and CorA proteins. Moreover, we also used the hydrophobic cluster analysis (HCA) for Alrp phylogeny, which allows a comparison among proteins with low similarity.

Materials and methods

Plasmid, strains and growth conditions

Genotypes of yeast strains used in this work are given in Table 1. All CM strains are isogenic derivatives of strain FY (Winston *et al.* 1995). The yeast strains and plasmid YCp*ALR1* [construction details c.f. Winston *et al.* (1995)] were kindly provided by Dr. Richard Gardner. Yeast was routinely grown on YPD (10 g l^{-1} yeast extract, 20 g l^{-1} bacto-peptone, 20 g l^{-1} glucose). The *alr1* mutants were supplemented with 0.25 M of $MgCl_2$ in the medium. Strain containing plasmid YCp*ALR1* was grown in synthetic complete minus uracil (SynCo-Ura) media (0.17 g l^{-1} yeast nitrogen base w/o amino acids and w/o ammonium sulfate, 5 g l^{-1} ammonium sulfate, and 20 g l^{-1} glucose with appropriate amino acids or/and bases added at 20 mg l^{-1} except for uracil). Their Cd^{2+} sensitivity was determined by the drop test. Yeast cultures in early stationary phase of growth (2 days in YPD media) were serially diluted (1:10 steps) and 10 μl from each dilution was plated on SynCo media supplemented with 0.4 mM of $CdCl_2$. Plates were photographed after 2 days of growth at 30 °C.

Table 1. Yeast strains employed in this study.

Strain	Genotype	Source
CM52	*MATα his3-Δ200 ura3-52 leu2-Δ202 trp1-Δ63 ALR1 ALR2*	MacDiarmid and Gardner (1998)
CM45	CM52, *alr1::HIS3*	MacDiarmid and Gardner (1998)
CM48	CM52, *alr2::URA3*	MacDiarmid and Gardner (1998)
CM66	CM52, *alr1::HIS3 alr2::URA3*	MacDiarmid and Gardner (1998)
ALKT-04	CM45, YCp*ALR1*	This study

Particle-induced X-ray emission (PIXE)

For the PIXE analysis, liquid media cultures were grown from a single colony for 2 days at 30 °C to a final density of about 2×10^8 cells ml^{-1}. The yeast cells were harvested by centrifugation, washed twice with 50 mM phosphate buffer (pH 6.0), resuspended in 10 ml of the same buffer (either containing or not 0.3 mM of $CdCl_2$) and then incubated at 30 °C for 24 h. The cells were then harvested by centrifugation and washed twice with ultrapure water and resuspended in 100 ml of the same water. The cell suspensions were fixed on filters with pores of 0.45 μm of diameter by vacuum filtration. The cell-containing filters and the blank control were mounted in a ring support for the PIXE measurements.

The PIXE analysis was carried out at the 3 MV Tandetron accelerator facility at the Physics Institute of the Federal University of Rio Grande do Sul, Brazil. All measurements were performed using a 2 MeV proton beam with an average current of 5 nA. The acquisition time for each sample was in the order of 10–20 min. The beam spot at the target position was about 9 mm^2. The filters containing the yeast cells, the blank filters, and the calibration targets were placed in a target holder, which accommodates up to 10 specimen. Each sample was positioned in the proton beam by means of an electric-mechanical system. The characteristic X-rays induced by the proton beam were detected by an HPGe detector from EG&G (GLP series, EG&G Ortec, CA, USA), with an energy resolution of 180 eV at 5.9 keV. The detector was positioned at 45° with respect to the beam axis. The electronics consisted of an Telennec245 amplifier associated with a PCA3 multichannel analyzer (Oxford Instruments, TN, USA) running in a PC-compatible computer. The GUPIX code (Maxwell *et al.* 1989) was used for data analysis.

Data mining for phylogenetic analysis

Two hundred and forty-five non-redundant primary protein sequences were obtained directly from GenBank hosted in the National Center for Biotechnological Information (NCBI) web page [http://www.ncbi.nlm.nih.gov/]. BLAST and PSI-BLAST (Altschul *et al.* 1997) programs were used for initial domain screening and comparison. All searches were made to saturation. From these 245 proteins we have chosen 17 CorA and Alr orthologous proteins for all subsequent phylogenetic analyses (Table 2).

Algorithms for sequence comparison

Global pair-wise multiple-alignments were performed with the aa sequences in the CLUSTALX 1.8 program (Thompson *et al.* 1994). The alignment parameters used were: gap open penalty 10.00; gap extension 0.20; sequences >10% diverged delayed; BLOSUM series matrix; residue-specific penalties on; and hydrophylic penalties on. When necessary, the alignments were manually adjusted using the BioEdit program (Hall 1999).

Algorithms for molecular phylogenetic inference

Phylogenetic and molecular evolutionary analyses were conducted using MEGA version 2.1 (Kumar *et al.* 2001). Neighbor-joining (NJ) method was used for phylogenetic tree searching and inference. The statistical reliability of the phylogenetic trees was tested by bootstrap analysis with 1000 replications. Moreover, the Poisson correction was applied in NJ for distance estimation. The complete deletion option was used in handling gaps or missing data obtained from the alignments.

Hydrophobic cluster analysis

Hydrophobic cluster analysis of selected sequences was performed as previously published (Gaboriaud *et al.* 1987) and consisted in displaying the primary protein structure on a duplicated alpha-helical net, where the hydrophobic residues are automatically contourned. These hydrophobic clusters correspond highly with the secondary protein structures and are extremely valuable for phylogenetic inferences when the protein sequences have a weak homology (<25% of identity/similarity) (Gaboriaud *et al.* 1987). The program DRAWHCA, used for this analysis, is available as a freeware at http://www.lmcp.jussieu.fr.

Table 2. Protein sequences used for HCA and phylogenetic analyses

Clade	Organims	Sequence	Abbreviation	Accession No.
CorA	*E. coli*	CorA	EcoCorA	gi|16131666|
	H. ducreyi	CorA	HduCorA	gi|33148114|
	H. hepaticus	CorA	HheCorA	gi|32267178|
	S. typhimurium	CorA	StyCorA	gi|16505746|
ZntB/Zntb-like				
	E. coli	ZntB(ydaN)	EcoZntB(ydaN)	gi|26108080|
	P. aeruginosa	ZntB	PaeZntB	gi|15596970|
	P. syringae	CmaX	PsyCmaX	gi|28869495|
	S. typhimurium	ZntB	StyZntB	gi|11878225|
	Y. pestis	ZntB	YpeZntB	gi|15980335|
Mrs2p				
	A. thaliana	Mrs2p-6	AthMrs2p-6	gi|25360918|
	H. sapiens	Mrs2p	HsaMrs2p	gi|10190702|
	R. norvegicus	Mrs2p	RnoMrs2p	gi|13027473|
	S. cerevisiae	Mrs2p	SceMrs2p	gi|171988|
Alrp				
	S. cerevisiae	Mnr2p	SceMnr2p	gi|486087|
	S. cerevisiae	Alr1p	SceAlr1p	gi|6324442|
	S. cerevisiae	Alr2p	SceAlr2p	gi|14318469|
	S. pombe	Alrp	SpoAlrp	gi|2853118|

Results and discussion

Phenotypic and PIXE analysis of S. cerevisiae *ALR and alr*Δ *mutants*

The drop test analysis performed with *ALR* wild-type and *alr1*Δ and *alr2*Δ single and double mutant strains is shown in Figure 1a and b. Strain CM45 (*alr1::HIS3 ALR2*) and strain CM66 (*alr1::HIS3 alr2::URA3*) had the highest sensitivity to $CdCl_2$ at a final concentration of 0.4 mM (Figure 1a), whereas strain CM48 (*alr2::URA3 ALR1*) showed tolerance to this Cd^{2+} concentration and survived as the WT strain CM52 (*ALR1 ALR2*). The WT and the *alr1::HIS3 ALR2* mutant harboring a single-copy *ALR1*-containing plasmid (ALKT-04) have the same $CdCl_2$ resistance (0.4 mM), confirming the full functionality of the plasmid-contained *ALR1* gene (Figure 1b).

The regulation of metal ion homeostasis in a cell is a very complicated process that relies on more than one metal transport protein and is highly regulated by transcription factors and protein turnover (Graschopf *et al.* 2001). The mechanisms regulating metal ion resistance in *S. cerevisiae* can be roughly classified in four

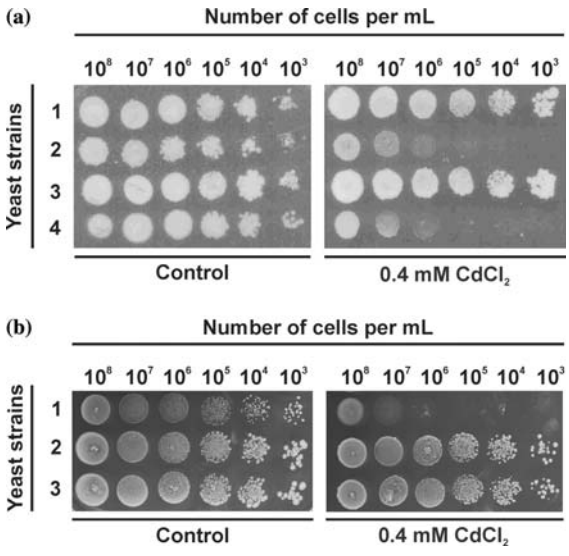

Figure 1. Sensitivity of *S. cerevisiae* to $CdCl_2$ (chronic exposure, Cd in the solid medium). (a) Control (no $CdCl_2$) and 0.4 mM $CdCl_2$ added. The number of cells per mL used in the drop test varied from 10^8 to 10^3. Yeast strains: 1. CM52 (*ALR1 ALR2*); 2. CM45 (*alr1::HIS3 ALR2*); 3. CM48 (*alr2::URA3 ALR1*) and 4. CM66 (*alr1::HIS3 alr2::URA3*). (b) Control (no $CdCl_2$) and 0.4 mM $CdCl_2$ added. The number of cells per mL used in the drop test varied from 10^8 to 10^3. Yeast strains: 1. CM45 (*alr1::HIS3 ALR2*); 2. ALKT-04 (*alr1::HIS3 ALR2* YCp*ALR1*); and 3. CM52 (*ALR1 ALR2*).

groups: (1) direct binding of metal ions by sulfur-containing aa or oligopeptides, (2) transcriptionally activated genes that provide metal ion binding proteins, (3) transmembrane pumps for thiol–metal ion complexes, and (4) proteins involved in proteolytic pathways (Perego & Howell 1997). Thus, a constellation of proteins, amino acids and oligopeptides with different functions can exert some effect in the metal ion homeostasis. Recently, using microarray and proteome analysis, it was shown that Cd^{2+} has a central role in the induction of sulfur-amino acid regulatory networks (Dormer *et al.* 2000) and also in the control of cellular glutathione and thioredoxin contents (Vido *et al.* 2001), indicating that Cd^{2+} may be sequestered by these sulfur-containing amino acids and peptides.

Taking all these factors into account, a good method in estimating intracellular cadmium is, therefore, necessary to correlate metal uptake and storage with regard to the above-described four groups. Cadmium can be easily determined by the PIXE technique, which allow us to correlate its quantity with toxicity of intracellularly accumulated metal ions. PIXE has been conventionally used to estimate metal contents in organic and inorganic materials (Kozai *et al.* 2003; Przybylowicz *et al.* 2003).

Thus, the stoichiometric ratio of metals in the yeast cells was estimated considering the cell density retained in the filter-membrane and the metal density calculated from the PIXE results expressed as ng cm^{-2} (g of cells)$^{-1}$. The Cd content determined in the yeast cells is shown in Figure 2. The results indicate that Cd is approximately four times more concentrated in the CM45 mutant (*alr1::HIS3 ALR2*) [1.60×10^5 ng cm^{-2} (g of cells)$^{-1}$] than in WT strain CM52 (*ALR1 ALR2*) [3.75×10^4 ng cm^{-2} (g of cells)$^{-1}$] or transformed ALKT-04 (*alr1::HIS3 ALR2* YCp*ALR1*) [4.00×10^4 ng cm^{-2} (g of cells)$^{-1}$]. This data also confirm the drop test results described above, indicating that the sensitivity of CM45 mutant is due to the elevated intracellular Cd^{2+} content.

The biological results indicate that Alr1p probably contributes to the cellular detoxification of Cd^{2+}. However, the previously published data on Alr1p indicated that the major function of this protein is to maintain the homeostasis of Mg^{2+}, and no evidence was given about its role in the detoxification of heavy metal ions. One tool that could be used to explain the biological results is based in a phylogenetic analysis

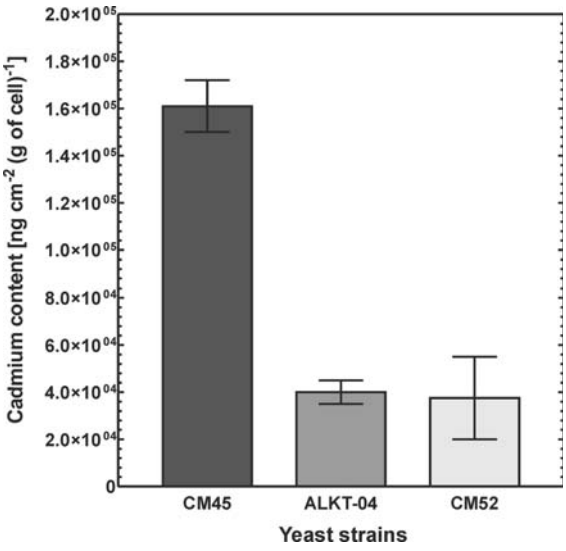

Figure 2. Cadmium content of yeast cells containing different copies of the *ALR1* gene by PIXE technique. Cd^{2+} taken up by yeast strains CM45 (*alr1::HIS3 ALR2*), ALKT-04 (*alr1::HIS3 ALR2* YCp*ALR1*), and CM52 (*ALR1 ALR2*). These values represent the average of three experiments. Cadmium concentrations are given in ng cm^{-2} (g of cells)$^{-1}$. For each sample, the uncertainty for the metal/cell ratio was estimated by taking into account the uncertainty in cell density of the sample and the fit uncertainty (%) given by the GUPIX code.

of the Alr proteins with those already described for metal ion homeostasis in other organisms.

Phylogenetic analysis of Alrp

To explain the biological data, we performed a comprehensive phylogenetic analysis of Alr proteins. Data mining using PSI-BLAST provided 245 proteins, and 17 proteins that show some degree of homology with those of *S. cerevisiae* and bacterial CorA have been studied. They were aligned and a corresponding global phylogenetic tree, based on NJ analysis was drawn (Figure 3). As described (MacDiarmid & Gardner 1998), the Alr1p and Alr2p sequences of *S. cerevisiae* are 70% identical. When these proteins were aligned with the Alrp sequence of *Schizosaccharomyces pombe*, the identity was 38%. We could also detect Alrp-like sequences in *Neurospora crassa* and *Candida albicans* (data not shown). The Alrp sequences show a high degree of homology with prokaryotic CorA, a protein family related to Mg^{2+} influx in bacteria and archaea, as well as with homologous proteins belonging to bacterial

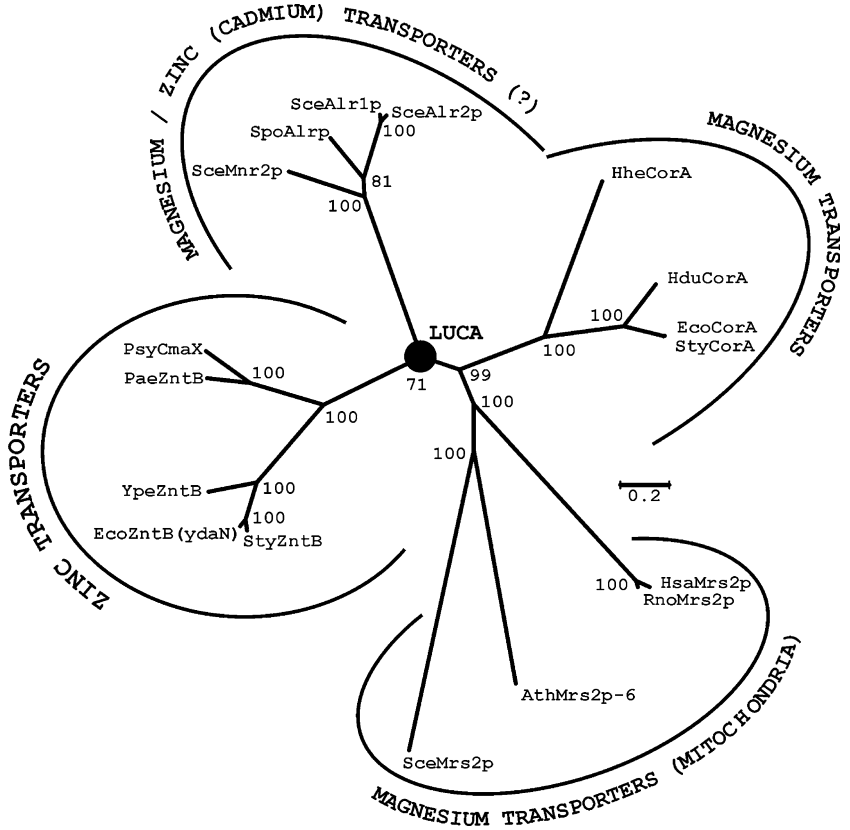

Figure 3. Unrooted phylogenetic tree obtained by neighbor-joining of selected protein sequences that share some degree of homology with CorA and Alrp. The four main clades and their biological function are indicated. The horizontal bar represents a distance of 0.2 substitutions per site and the bootstrapping numbers are indicated at the nodes. The common ancestor between ZntB proteins and Alrp is shown within a solid circle. Abbreviation: last universal common ancestor (LUCA).

zinc transporters (ZntB and CmaX proteins) and Mrs2 proteins (related to mitochondrial Mg^{2+} influx/efflux). In a global phylogenetic perspective, these proteins compose four distinct groups or clades: (i) eukaryotic Alrp sequences, (ii) prokaryotic CorA, (iii) prokaryotic ZntB/ZntB-like sequences, and (iv) mitochondrial Mrs2p (CorA-like) sequences (Table 2). However, the strong orthology observed between the prokaryotic ZntB/ZntB-like sequence and eukaryotic Alrp sequences (Figure 3) suggests a more detailed evolutive analysis of this relationship.

Our phylogenetic data were refined by selecting some representative protein sequences for each clade and performing a HCA analysis. HCA is a sensitive method of sequence comparison that detects two- and three-dimensional similarities between protein domains showing very limited aa relatedness, typically below the so-called "twilight zone" (25–30%) (Gaboriaud *et al.* 1987). In our case, the HCA was able to detect similarities of hydrophobic clusters between the clades (Figure 4). All analysed proteins are composed by two Alrp/CorA-characteristic transmembrane domains (TMD1 and TMD2) located in the polypeptide C-termini (Kehres *et al.* 1998). These TMDs are connected by a conserved short loop with a canonical sequence (Y/F)GMN (LOOP). Moreover, these proteins show a long amino-terminus region located into the cytoplasm, whose function and/or role in the mechanism of divalent cation transport is largely unknown (Smith *et al.* 1993). Interestingly, only the CorA proteins show a third TMD located close to the conserved TMD1 and TMD2 (Figure 4). This putative transmembrane domain has been previously described by Smith *et al.* (1993) but its role for metal transport was not analysed until now.

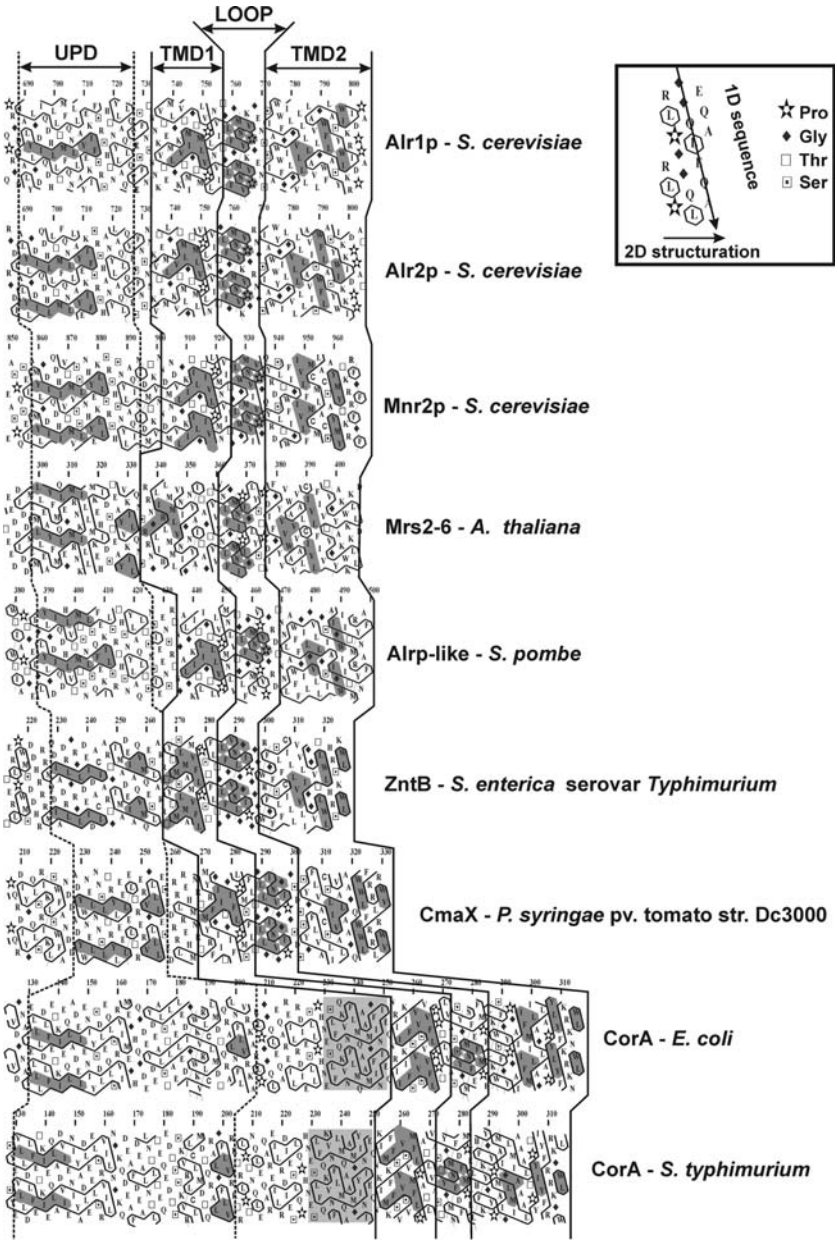

Figure 4. Hydrophobic cluster analysis of eukaryotic Alr, Mnr2, and Mrs2 proteins with prokaryotic ZntB/CmaX and CorA sequences. Vertical lines indicate domains shared between all proteins. The way to read the sequence and special symbols are indicated in the inset. Conservation of hydrophobic clusters are indicated by a light gray shade. The dark gray box in CorA sequences represents the proposed third transmembrane domain. Abbreviations: transmembrane domains 1/2 (TMD1/2), unknown protein domain (UPD), conserved loop sequence (LOOP).

Comparing all sequences by HCA (Figure 4), it becomes clear that the Alrp and Mnr2p of *S. cerevisiae* show a high similarity of C-terminal secondary structures. The phylogenetic data support the hypothesis that Alrp and Mnr2p are paralogous proteins with similar functions.

The mitochondrial Mrs2p of yeast, metazoa and *Arabidopsis thaliana* also show an extremely conserved TMD and protein loop with Alrp, corroborating the role of this family in the mitochondrial Mg^{2+} transport in addition to its function in RNA splicing (Gregan *et al*. 2001). It is

known that Mrs2p plays a role in the influx and efflux of Mg^{2+} in the yeast mitochondria (Kolisek *et al.* 2003), and that it can fully substitute human mitochondrial Mrs2p (Zsurka *et al.* 2001). In *A. thaliana*, Li et al. (2001) described a 10-member protein family consisting of multiple paralogous Mnr2p, showing that these proteins have special functions in magnesium homeostasis in higher plants. Our phylogenetic results also show that both Mrs2p and CorA proteins compose an orthologous group, both sharing a recent common ancestor (Figures 3 and 4). These analyses indicate that Mrs2p has a prokaryotic origin which evolved into a specialized Mg^{2+} transporter system in eukaryotic mitochondria. Moreover, the overexpression of a *CorA* gene can functionally substitute a disrupted *mrs2* gene in yeast, thus corroborating our results (Bui *et al.* 1999).

The conservation of TMD1 and TMD2 could also be seen between fungal Alrp, ZntB protein of *Salmonella enterica*, and CmaX protein of *Pseudomonas syringae*. The ZntB and ZntB-like proteins (CmaX) are specific for zinc efflux in prokaryotes. The ZntB protein was previously characterized in *Salmonella enterica* serovar Typhimurium (Worlock & Smith 2002). Malfunctions of this protein leads to increased sensitivity to cytotoxic levels of Cd^{2+} and Zn^{2+} and to a reduced capacity of zinc efflux. ZntB and ZntB-like proteins as well as fungal Alrp have an unusual structure for a transport protein since they are relatively small and possess only a single membrane domain of minimal size (Caldwell & Smith 2003). Zn^{2+} homeostasis in yeast is accomplished by several proteins that can be grouped in high and low affinity-uptake systems, transcriptional activators and vacuole zinc transporters (MacDiarmid *et al.* 2000). The high affinity Zn^{2+} uptake system, characterized by gene *ZRT1*, is also responsible for the uptake of extracellular Cd^{2+} and *zrt1* mutants showing low levels of intracellular Cd^{2+} (Gomes *et al.* 2002). Thus, with both Alrp and ZntB/ZntB-like proteins sharing a common ancestor as indicated by sequence comparison and HCA (Figures 3 and 4), and considering the biological results obtained by the drop test and PIXE (Figures 1 and 2), it may be argued that Alrp have a specialized role in the detoxification of intracellular cadmium when the cell lives in a Cd^{2+}-rich environment.

The HCA data also show the presence of a third domain situated upstream of TMD1 (Figure 4) which we named unknown protein domain (UPD). The secondary structure analysis of UPD indicates that it is composed of a conserved α-helix motif, but a comprehensive transmembrane analysis of UPD by the dense alignment surface (DAS) method (Cserzo *et al.* 1997) indicates that this α-helix motif is not a potential transmembrane domain (data not shown). It will be interesting to analyse the potential role of this UPD in the divalent metal ion transport.

A model for Cd^{2+} detoxification by Alrp in S. cerevisiae

The integration of phylogenetic analyses and biological data clearly suggests that Alrp acts in the heavy metal detoxification of the cell, though only the more specific function of Alrp in the cellular Mg^{2+} influx/efflux has been proven (Liu *et al.* 2002). When a WT cell is present in a Cd- or even in a Zn-rich environment (Figure 5a), as it is the case of CM52 strain (*ALR1 ALR2*), some transmembrane pumps take up these heavy metals that inside the cell promptly react with two molecules of glutathione (GSH), generating bis(glutathionato)cadmium [$(GS)_2Cd$] and, probably, bis(glutathionato)zinc [$(GS)_2Zn$]. These transmembrane pumps, e.g. Zrt1p, act as high affinity zinc transporters, but can also transport Cd^{2+} if it is present in elevated concentrations (Gomes *et al.* 2002). Moreover, some divalent metal low-affinity transmembrane proteins (LAp), e.g. Bsd2p and Zrt2p of *S. cerevisiae* and Irt1p of *A. thaliana*, can also transport heavy metals, especially Zn^{2+}, under stress conditions (Zhao & Eide 1996; Perego & Howell 1997). Thus, the presence of these cytosolic transmembrane proteins allows uptake of heavy metals from the environment. However, as mentioned above, a WT cell has several detoxification mechanisms. One of these is offered by vacuolar transmembrane proteins, binding the [$(GS)_2Cd$] conjugate and sequestering it into the vacuole (Figure 5a). The best-characterized member of this group is Ycf1p, a *S. cerevisiae* ATP-binding cassete (ABC) protein that is energized by Mg^{2+} and ATP. Ycf1p was shown to transport organic glutathione-conjugates and also the [$(GS)_2Cd$] complex (Li *et al.* 1997). Moreover, mutations in this protein render yeast hypersensitive to Cd^{2+} (Perego & Howell 1997). Also belonging to this group, Bpt1p, a paralogue ABC transporter of Ycf1p in

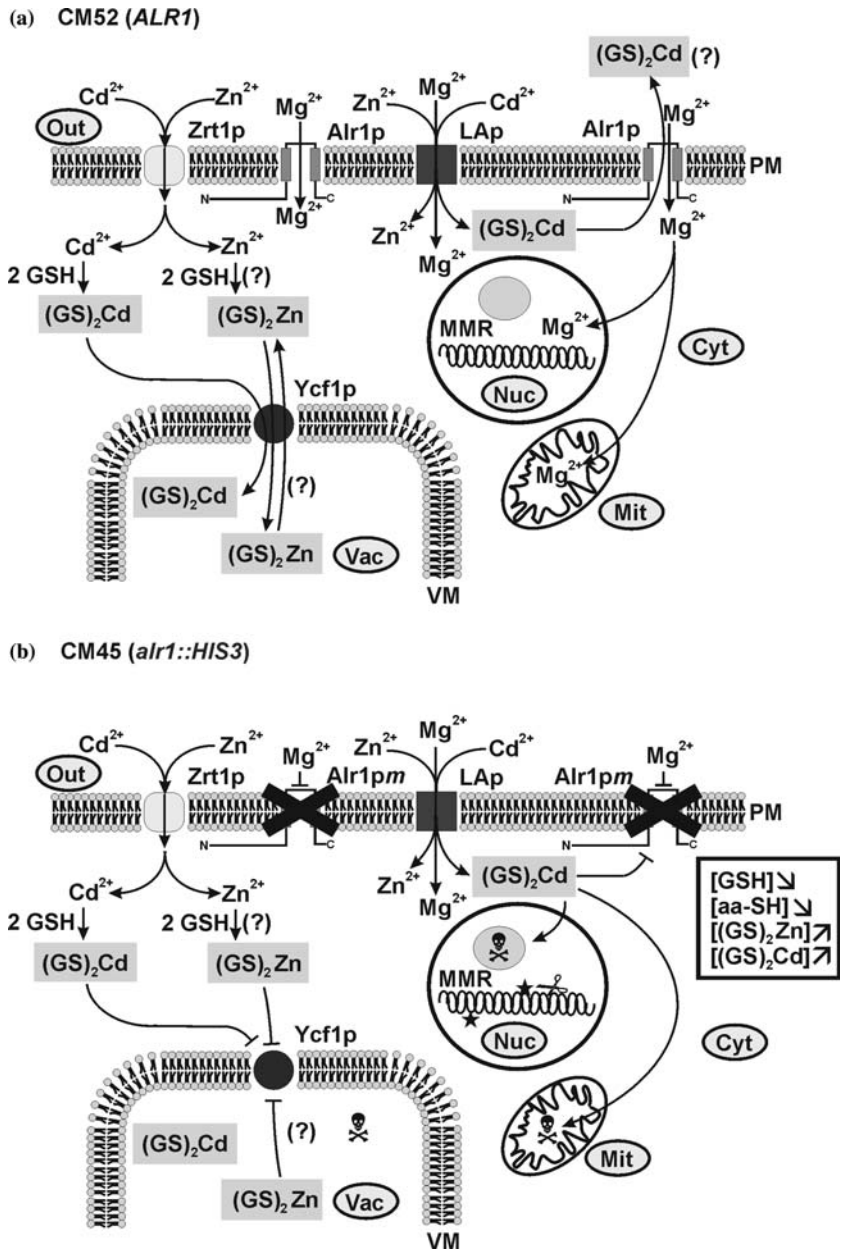

Figure 5. Model proposed for Alrp function in *S. cerevisiae* in a rich Cd^{2+} and Zn^{2+} environment. In WT (CM52), as represented in (a), both Cd^{2+} and Zn^{2+} are taken up by known transmembrane proteins, e.g. Zrt1p and low-affinity proteins (LAps). Cd^{2+} and probably Zn^{2+} react with glutathione (GSH), generating $[(GS)_2Cd]$ and $[(GS)_2Zn]$, respectively. These complexes are transported into the vacuole by the Ycf1p or excreted by Alrp (represented by Alr1p). Alrp itself is a high-affinity transmembrane protein related to the Mg^{2+} influx, maintaining the Mg^{2+} homeostasis for nuclear and mitochondrial metabolic functions. LAps also act in the Mg^{2+} homeostasis, but with lower efficiency. However, a deleterious mutation in Alrp (Alr1p*m*), as shown in (b), allows an increase in the accumulation of $[(GS)_2Cd]$ and $[(GS)_2Zn]$ complexes, as indicated in the inset. These complexes induce a shutdown of glutathione and thiol-compounds (inset), perturbing the redox metabolism (e.g. oxidized DNA bases, as represented by stars in the model). These Cd^{2+}, $[(GS)_2Cd]$ and $[(GS)_2Zn]$ concentrations also inhibit Ycf1p, as well as DNA mismatch repair enzymes (MMR) and mitochondrial functions. Finally, nucleases act on nuclear DNA (represented by a scissor) leading to cell death (bones-and-skull representation). Abbreviations: extracellular environment (Out), nucleous (Nuc), mitochondria (Mit), cytoplasm (Cyt), plasma membrane (PM), vacuole membrane (VM). The symbol (?) stands for a putative pathway. Alr1p is represented with its N- and C-termini.

yeast, takes part in the process of Cd^{2+} detoxification (Klein *et al.* 2002). In all cases, a Alrp protein-guaranteed Mg^{2+} homeostasis is necessary for the correct function of protein-dependent Cd^{2+} detoxification. A deleterious mutation in Alrp (e.g. CM45) leads to a lethal phenotype in a rich Cd^{2+} environment (Figure 5b). A first explanation for this process would be that the uptake of Mg^{2+} from the outside has become less efficient in the *alr1* mutant strain and the cell has used the LAp for this function. The deficiency in Mg^{2+} could also shutdown the ABC vacuolar transport systems and cause accumulation of the $[(GS)_2Cd]$ conjugate, possibly depleting glutathione, therefore elevating the general concentration of Cd^{2+} in the cell that enters via Zrt1p and LAp transporters. However, in an environment containing high concentration of Mg^{2+}, as used in our experiments, the Alr1p mutants and WT have approximately the same amount of intracellular Mg^{2+} (Graschopf *et al.* 2001). Therefore, we must conclude that the problem of Cd^{+2} toxicity in yeast *alr1* mutants cannot be reduced to a simple deficiency of intracellular Mg^{2+}. Alternatively, if Alrp and ZntB proteins really share a common ancestor as was suggested in our work, Alrp might also serve as a Cd^{2+} efflux system. We can thus speculate that a deficiency in this mechanism increases the intracellular pool of Cd^{2+} and $[(GS)_2Cd]$, leading to a vacuolar saturation with Cd^{2+} and an inhibition of thiol-dependent redox systems (Figure 5b) (Dormer *et al.* 2000; Vido *et al.* 2001). In that case, without the Alrp to export the excess of Cd^{2+} or $[(GS)_2Cd]$ outside the cell, all cellular systems become unstable (McMurray & Tainer 2003). In particular, the DNA mismatch repair system is strongly inhibited by Cd^{2+} (McMurray & Tainer 2003) and more Cd^{2+} and $[(GS)_2Cd]$-induced oxidized bases accumulate in mitochondrial and nuclear genomes (Figure 5b). Ultimately, the elevated generation of reactive oxygen species associated with functional alterations in DNA repair systems, the activation of DNA nucleases and caspase-related protease would lead the cells into apoptosis (Madeo *et al.* 1999, 2002). Biological data support this catastrophic scenario, but more analyses are needed to confirm the potential of Cd^{2+} to induce a programmed cell death in yeast. The model allows us to speculate that Zn^{2+} could react with GSH, generating $[(GS)_2Zn]$. Since the detoxification pathway for $[(GS)_2Zn]$ is similar to that for $[(GS)_2Cd]$, elevated concentrations of Zn^{2+} in an *alr1*Δ background could induce Cd^{2+}-like cytotoxicity.

PIXE technique coupled to refined phylogenetic analyses (e.g. HCA) of protein sequences related to metal transporters are valuable tools in elucidating the role of cellular heavy metal detoxification systems. However, the overall picture of Cd^{2+} metabolism as that of other heavy metals in eukaryotic cells is still a challenge to our understanding.

Acknowledgements

We thank Dr. Richard Gardner for providing the *Saccharomyces cerevisiae* strains and plasmids. We also thank Dr. Augusto Schrank for discussion and helpful comments on the manuscript. Contract/grant sponsor: FAPERGS, CAPES, GENOTOX laboratory.

References

Altschul SF, Madden TL, Schäffer AA *et al.* 1997 Gapped BLAST and PSI-BLAST: the new generation of protein database search programs. *Nucleic Acids Res* **25**, 3389–3402.

Brennan RJ, Schiestl RH. 1996 Cadmium is an inducer of oxidative stress in yeast. *Mutat Res* **356**, 171–178.

Bui DM, Gregan J, Ragnini A, Schweyen RJ. 1999 The bacterial magnesium transporter *CorA* can functionally substitute for its putative homologue Mrs2p in the yeast inner mitochondrial membrane. *J Biol Chem* **274**, 20438–20443.

Caldwell AM, Smith RL. 2003 Membrane topology of the ZntB efflux system of *Salmonella enterica* serovar Typhimurium. *J Bacteriol* **185**, 374–376.

Cserzo M, Wallin E, Simon I, von Heijne G, Elofsson A. 1997 Prediction of transmembrane alpha-helices in procariotic membrane proteins: the Dense Alignment Surface method. *Prot Eng* **10**, 673–676.

Dormer UH, Westwater J, McLaren NF, Kent NA, Mellor J, Jamieson DJ. 2000 Cadmium-inducible expression of the yeast *GSH1* gene requires a functional sulfur-amino acid regulatory network. *J Biol Chem* **275**, 32611–32616.

Eide D, Guerinot ML. 1997 Metal ion upake in eukaryotes: research on *Saccharomyces cerevisiae* reveals complexity and insights about other species. *ASM News* **63**, 199–205.

Gaboriaud C, Bissery V, Benchetrit T, Mornon JP. 1987 Hydrophobic cluster analysis: an efficient new way to compare and analyse amino acid sequences. *FEBS Lett* **224**, 149–155.

Gomes DS, Fragoso LC, Riger CJ, Panek AD, Eleutherio ECA. 2002 Regulation of cadmium uptake by *Saccharomyces cerevisiae*. *Biochim Biophys Acta* **1573**, 21–25.

Graschopf A, Stadler JA, Hoellerer MK *et al.* 2001 The yeast plasma membrane protein Alr1 controls Mg^{2+} homeostasis and is subject to Mg^{2+} dependent control of its synthesis and degradation. *J Biol Chem* **276**, 16216–16222.

Gregan J, Kolisek M, Schweyen RJ. 2001 Mitochondrial Mg^{2+} homeostasis is critical for group II intron splicing in vivo. *Genes Dev* **15**, 2229–2237.

Hall TA. 1999 BioEdit: a user-friendly biological sequence alignment editor and analysis program for Windows 95/98/NT. *Nucl Acids Symp Ser* **41**, 95–98.

Kehres DG, Lawyer CH, Maguire ME. 1998 The *CorA* magnesium transporter gene family. *Microb Comp Genomics* **3**, 151–169.

Klein M, Mamnun MY, Eggmann T *et al*. 2002 The ATP-binding cassete (ABC) transporter Bpt1p mediates sequestration of glutathione conjugates in yeast. *FEBS Lett* **520**, 63–67.

Kolisek M, Zsurka G, Samaj J, Weghuber J, Schweyen RJ, Schweigel M. 2003 Mrs2p is an essential component of the major electrophoretic Mg^{2+} influx system in mitochondria. *EMBO J*. **22**, 1235–1244.

Kozai N, Ohnuki T, Komarneni S *et al*. 2003 Uptake of cadmium by synthetic mica and apatite: observation by micro-PIXE. *Nucl Instrum Meth B* **210**, 513–518.

Kumar S, Tamura K, Jakobsen IB, Nei M. 2001 MEGA2: *Molecular Evolutionary Genetics Analysis software*. Tempe, Arizona, USA, Arizona State University.

Li Z-S, Lu Y-P, Zhen R-G, Szczypka M, Thiele DJ, Rea PA. 1997 A new pathway for vacuolar cadmium sequestration in *Saccharomyces cerevisiae*: YCF1-catalized transport of bis(glutathionato)cadmium. *Proc Natl Acad Sci USA* **94**, 42–47.

Li L, Tutone AF, Drummond RS, Gardner RC, Luan S. 2001 A novel family of magnesium transport genes in *Arabidopsis*. *Plant Cell* **13**, 2761–2775.

Liu GJ, Martin DK, Gardner RC, Ryan PR. 2002 Large Mg^{2+}-dependent currents are associated with the increased expression of *ALR1* in *Saccharomyces cerevisiae*. *FEMS Microbiol Lett* **10574**, 1–7.

MacDiarmid CW, Gaither LA, Eide D. 2000 Zinc transporters that regulates vacuolar zinc storage in *Saccharomyces cerevisiae*. *EMBO J* **19**, 2845–2855.

MacDiarmid CW, Gardner RC. 1998 Overexpression of *the Saccharomyces cerevisiae* magnesium transport system confers resistance to aluminium ion. *J Biol Chem* **273**, 1727–1732.

Madeo F, Fröhlich E, Ligr M *et al*. 1999 Oxygen stress: a regulator of apoptosis in yeast. *J Cell Biol* **145**, 757–767.

Madeo F, Herker E, Maldener C *et al*. 2002 A caspase-related protease regulates apoptosis in yeast. *Mol Cell* **9**, 911–917.

Maxwell JA, Campbell JL, Teesdale WJ. 1989 The GUELPH PIXE software package. *Nucl Instrum Meth B* **43**, 218–230.

McMurray CT, Tainer JA. 2003 Cancer, cadmium and genome integrity. *Nat Genet* **34**, 34239–34241.

Moeller T, Bailar JC, Kleinberg J, Guss CO, Castellion ME, Metz C. 1984 *Chemistry with Inorganic Qualitative Analysis*. Orlando: Academic Press, Inc.; p. 929.

Perego P, Howell SB. 1997 Molecular mechanisms controlling sensitivity to toxic metal ion in yeast. *Toxicol Appl Pharmac* **147**, 312–318.

Pfeiffer J, Guhl J, Waidner B, Kist M, Bereswill S. 2002 Magnesium uptake by CorA is essential for viability of the gastric pathogen *Helicobacter pylori*. *Infect Immun* **70**, 3930–3934.

Pinã RG, Cervantes C. 1996 Microbial interactions with aluminium. *Biometals* **9**, 311–316.

Przybylowicz WJ, Przybylowicz JM, Migula P, Glowacka E, Nakonieczny M, Augustyniak M. 2003 Functional analysis of metals distribution in organs of the beetle *Chrysolina pardalina* exposed to excess of nickel by Micro-PIXE. *Nucl Instrum Meth B* **210**, 343–348.

Smith RL, Banks JL, Snavely MD, Maguire ME. 1993 Sequence and topology of the CorA magnesium transport system of *Salmonella typhimurium* and *Escherichia coli*. *J Biol Chem* **268**, 14071–14080.

Stohs SJ, Bagchi D. 1995 Oxidative mechanisms in the toxicity of metal-ions. *Free Radic Biol Med* **18**, 321–336.

Thompson JD, Higgins DG, Gibson TJ. 1994 CLUSTAL W: improving the sensitivity of progressive multiple sequence alignment through sequence weighting, positions-specific gap penalties and weight matrix choice. *Nucleic Acids Res* **22**, 4673–4680.

Tomsett AB, Thurman DA. 1988 Molecular biology of metal tolerance of plants. *Plant Cell Environ* **11**, 383–394.

Trevors J, Stratton GW, Gadd GM. 1986 Cadmium transport resistance and toxicity in bacteria, algae and fungi. *Can J Microbiol* **32**, 126–131.

Vido K, Spector D, Lagniel G, Lopez S, Toledano MB, Labarre J. 2001 A proteome analysis of the cadmium response in *Saccharomyces cerevisiae*. *J Biol Chem* **276**, 8469–8474.

Winston F, Dollard C, Ricupero-Hovasse SL. 1995 Construction of a set of convenient *Saccharomyces cerevisiae* strains that are isogenic to S288C. *Yeast* **11**, 53–55.

Worlock AJ, Smith RL. 2002 ZntB in a novel Zn^{2+} transporter in *Salmonella enterica* serovar Typhimurium. *J Bacteriol* **184**, 4369–4373.

Zhao H, Eide D. 1996 The *ZRT2* gene encodes the low affinity zinc transporter in *Saccharomyces cerevisiae*. *J Biol Chem* **271**, 23203–23210.

Zsurka G, Gregan J, Schweyen RJ. 2001 The human mitochondrial Mrs2 protein functionally substitutes for its yeast homologue, a candidate magnesium transporter. *Genomics* **72**, 158–168.